KINETIC MEASURES FOR DISTINGUISHING VULNERABLE FROM STABLE ATHEROSCLEROTIC PLAQUE WITH DYNAMIC CONTRAST-ENHANCED MRI

Zengchang Qin [†] *Yaping Wang* [†] *Wanshu Zhang*[§] *Jianhui Chen*[‡] *Tao Wan*[§*]

[†] Intelligent Computing & Machine Learning Lab, School of ASEE, Beihang University, China
[‡] No. 91 Central Hospital of PLA, Henan, China
[§] School of Biological Science and Medical Engineering, Beihang University, China

ABSTRACT

Carotid atherosclerosis is a primary cause of stroke, which is responsible for a majority of disabilities and deaths worldwide. Plaque inflammation and abundant microvasculature have been identified as important aspects contributing to plaque vulnerability that can be studied non-invasively with dynamic contrast-enhanced magnetic resonance imaging (DCE-MRI). Due to the asymptomatic nature of vulnerable plaque, there is an unmet clinical need to identify and characterize these lesions before they rupture. We presented an automated computerized method based on kinetic measures to distinguish vulnerable from stable atherosclerotic plaques on DCE-MRI. Four classes of kinectic features, including pharmacokinetic, intensity kinetic, histogram kinetic, and textual kinetic features, were extracted for capturing the pathophysiologic changes in various aspects of plaque vascular structure and functionality in atherosclerosis. These features can reflect the local inflammatory processes and microvasculature changes appearing in plaque destabilization. Our method was evaluated on real clinical data and achieved the area under the curve of 0.95 using a combined feature set, suggesting a potential of this method applied to a computer-aided diagnosis system for an early detection of vulnerable plaques.

Index Terms— Carotid atherosclerosis, plaque, DCE-MRI, kinetic measure.

1. INTRODUCTION

Atherosclerosis is a diffuse, degenerative disease of the arteries resulting in the formation of plaques in the vessel wall, which can cause stenosis, embolization, and thrombosis. Atherosclerotic plaques have been characterized as stable and vulnerable. Ruptures of vulnerable plaques can eventually induce thrombus formation in the lumen. The luminal obstruction of carotid arteries is an increased risk for a stroke, which is also the leading cause of death worldwide [1]. However, carotid atherosclerosis symptoms are often unnoticed especially during its initial stage. As vulnerable carotid atherosclerotic plaques are high-risk and often unrecognized before clinical events, such as stroke, identification of a culprit lesion before it ruptures remains a challenging task [2].

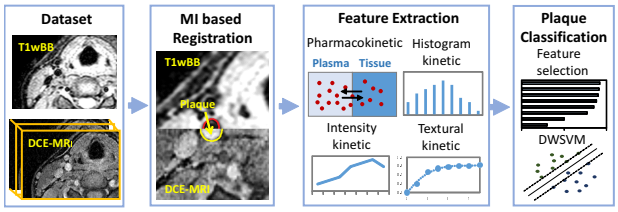

Fig. 1. The flowchart shows that the presented method comprised three main modules to distinguish vulnerable and stable plaques.

Recently, dynamic contrast-enhanced magnetic resonance imaging (DCE-MRI) has been used extensively to study neovasculature volume in carotid atherosclerotic plaque, which allows a kinetic analysis of contrast agent uptake in tissues of interest [1]. For instance, Chen *et al.* [3] utilized pharmacokinetic (PK) modeling to evaluate temporal changes on DCE-MRI for early atherosclerotic lesion assessment in a rabbit model. Our previous work [2] aimed at developing a spatio-temporal texture based method for distinguishing vulnerable versus stable plaques on DCE-MRI using a rabbit model of atherothrombosis. Gaens *et al.* [4] compared four known PK models and found the Patlak model [5] was suitable for describing carotid plaque enhancement. All these methods either applied to the rabbit model or focused on physiological kinetic parameters to characterize carotid atherosclerotic plaque. The purpose of this work is to investigate discrimination capability of various kinetic measures on DCE-MRI in stratifying vulnerable and stable plaques with human data.

We presented an automated computerized method for distinguishing vulnerable from stable atherosclerotic plaque with DCE-MRI using multiple kinetic features. The method was evaluated using real clinical data cohort. The methodology consisted of three main modules as illustrated in the

* Corresponding author's e-mail: taowan@buaa.edu.cn (T.Wan). This work was partially supported by the National Natural Science Foundation of China under award No. 61401012.

flowchart shown in Figure 1. In feature extraction, we computed four types of image-based kinetic measures, including pharmacokinetic, intensity kinetic (IK), histogram kinetic (HK), and textual kinetic (TK) features. PK feature provides a physiologic interpretation of DCE-MRI. IK represents intensity variation during contrast enhancement within plaque. HK features (i.e., dynamic histogram of oriented gradients (DHoG) and dynamic local binary patterns (DLBP)) allow for construction of unique plaque signatures that capture the frequency of occurrence of different spatio-temporal textural patterns on DCE-MRI. TK characterizes subtle textural changes in contrast uptakes. A combination of these four classes of kinetic measures provides a comprehensive set of features to characterize the pathophysiologic changes in various aspects of plaque vascular structure and functionality in atherosclerosis.

The remainder of this paper is organized as follows. The dataset description and methods are described in Section 2. The experimental results and discussion are demonstrated in Section 3. Section 4 concludes the paper.

2. MATERIALS AND METHODS

2.1. Dataset Description

The image data were retrospectively collected from the China's No. 91 Central Hospital of PLA using a 3T MR scanner (Achieva; Philips, Best, The Netherlands) with a seven-channel coil. A total of 22 DCE-MRI and $T1$-weighted black blood (T1wBB) sequences were obtained from 22 subjects (14 male subjects; 8 female subjects; mean age ($\pm$ standard deviation) of 49.8 ± 23.3 years) who have been diagnosed with 50% stenosis underwent diagnostic angiography for suspected carotid artery disease between 2012 and 2014. All the cases were anonymised. For each patient study, a radiologist with more than 15 years of experience manually delineated the vessel outer wall and lumen contour of each carotid plaque on a representative frame of the DCE-MRI sequence and associated T1wBB slide. In total, 16 vulnerable and 20 stable plaques were utilized in this study. DCE-MRIs were acquired before and every 19-27 seconds after injection of 0.1 mmol/kg of a gadolinium-based contrast agent at rate of 2 ml/second by a power injector.

2.2. Image Preprocessing

Because the manual delineations of vessel outer wall and lumen were performed on DCE-MRI and T1wBB, respectively, a registration method based on the maximization of mutual information (MI) was utilized to align corresponding DCE-MRI and T1wBB [6]. A 2D affine transformation ($X^{'} = s \cdot \mathbf{R} \cdot X + b$, s, $\mathbf{R}$, b are the scale factor, rotation matrix, and translation vector.) was adopted to register the image pair in both global and local forms, allowing registration for entire image and local deformation. The interpolation method, which was used to calculate intensities on the deformed moving image, was bilinear interpolation. MI was utilized as a similarity measure to drive transformation optimization.

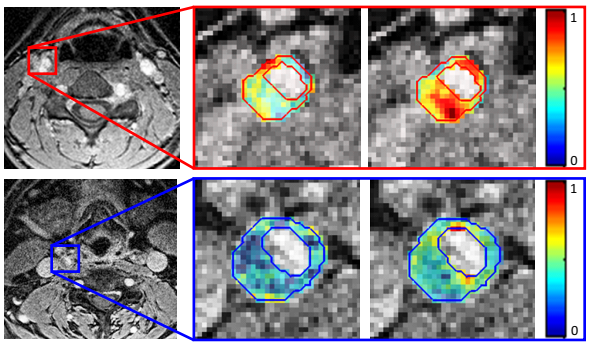

Fig. 2. Two examples of PK features (K^{trans}, v_p) for a vulnerable plaque (first row) and a stable plaque (second row). The color-coded feature images suggested a higher internal heterogeneity for vulnerable case. The original images are post-contrast with peak enhancement.

2.3. Feature Extraction

Four types of features, including pharmacokinetic features, intensity kinetic features, histogram kinetic features, and textural kinetic features were extracted to characterize plaques.

2.3.1. Pharmacokinetic features

The PK models (e.g., Patlak's PK model [5]) are most commonly used in DCE-MRI to provide a physiologic interpretation of image sequence via two parameters, i.e., K^{trans} (the transfer constant between the plasma and tissue compartments), and v_p (the blood plasma volume fraction). The concentration of the contrast agent in tissue $C_t(T)$ can be defined as:

$$C_t(T) = v_p C_p(T) + K^{\text{trans}} \int_0^T C_p(t)dt, \qquad (1)$$

where $C_p(t)$ is the concentration of the contrast agent in blood plasma. To exclude nonphysical solutions, the parameter v_p was constrained to a maximum of 1. The key step for the PK model was to precisely compute $C_p(t)$. Due to the small size of vessels and plaques, we estimated $C_p(t)$ through finding the optimal pixel intensity curve via a mean-shift method [7], in which the cluster center of signal intensity curve was iteratively determined by moving the center to the sample mean of the previous point, most likely to be associated with arterial blood. $C_p(t)$ was further corrected by [8]:

$$C_p(t) = \frac{A}{\sigma\sqrt{2\pi}} e^{\frac{-(t-T)^2}{2\sigma^2}} + \frac{\alpha e^{-\beta t}}{1 + e^{-s(t-\tau)}} \qquad (2)$$

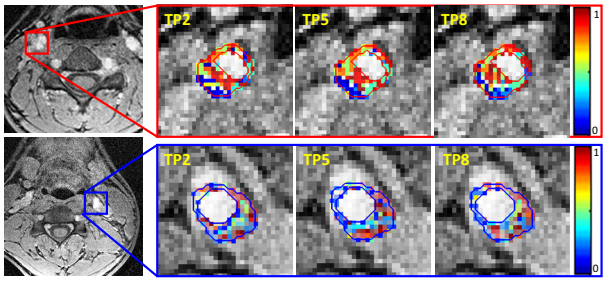

Fig. 3. Two examples of DLBP features for a vulnerable plaque (first row) and a stable plaque (second row) at three time points (TP). The color-coded feature images indicated a higher heterogeneity in contrast enhancement patterns along DCE-MRI time series for vulnerable plaque.

where A, T, and σ are the scaling constant, center, and width of the Gaussian, respectively. α and β are the amplitude and decay constant of the exponential, s and τ are the width and center of the sigmoid. Figure 2 illustrates two examples of vulnerable and stable plaques. The color-coded texture images suggested a higher heterogeneity in enhancement patterns for vulnerable plaque compared to stable case.

2.3.2. Intensity kinetic features

Plaque enhancement can be qualitatively characterized by assessing the enhancement curve obtained by plotting the signal intensity values over time after contrast injection. Different from the traditional enhancement kinetic analysis by computing maximal uptake, time to peak, uptake rate, and washout rate [9], we measured the following three IK features: (1) Discrete Fourier transform (DFT) coefficients [10] based on a 1D pixelwise DFT on enhanced signal intensity curve to represent the frequency content of the corresponding temporal enhancements; (2) The area under curve (AUC) to describe the retention of contrast agent within plaque; (3) The peak of the first derivative of enhance curve over the time course to measure the update of contrast agent [11]. These attributes are less sensitive to noise, allowing effective measures of contrast enhancement patterns within the plaques.

2.3.3. Histogram kinetic features

We computed two types of histogram kinetic features, i.e., dynamic histogram of oriented gradients and dynamic local binary patterns [12].

DHoG: We computed multi-resolution based DHoG to describe the dynamic texture changes in gradient orientation during the contrast enhancement. The local texture in plaque was captured by the distribution over edge orientations within a small region, while the spatial contextual information is obtained by tiling the image into regions at multiple resolutions. The basic steps for computing DHoG are as follows:

(1) A gradient image $G(t), t \in \{0, 1, ..., T-1\}$ was obtained via a gradient filter $[-1, 0, 1]$ applied on both horizontal and vertical directions of image slide. The plaque region was divided into small blocks at resolution level k, $k \in \{1, ..., K\}$;
(2) Each pixel p in examined block $B_{k,j}$, $j \in \{1, ..., V\}$, calculated a weighted vote $w(p)$ based on the orientation of the gradient element centered on it;
(3) The temporal HoG vector $H_{k,j,N}$ was computed for each grid block $B_{k,j}$ across the time points and quantized into N orientation bins. The DHoG feature for DCE-MRI time series is a concatenation of all $H_{k,j,N}$, $k \in \{1, ..., K\}$, $j \in \{1, ..., V\}$.

DLBP: The DLBP features reflect regional heterogeneity and texture changes within the plaques over time after contrast injection (see Figure 3). Similar to the DHoG, the DLBP was implemented in a multi-resolution fashion. For image at time point t, plaque region was divided into multiple blocks $B_{k,j}$, $j \in \{1, ..., V\}$ at resolution level k, $k \in \{1, ..., K\}$. For each pixel $p \in B_{k,j}$, compared the pixel to each of its 8 neighbors, which gave an 8-digit binary number for this pixel. A temporal LBP $P_{k,j,N}$ over the cell was then computed by accumulating all 8-digit binary numbers within this cell along the time point $t \in \{0, 1, ..., T-1\}$. The temporal LBP was normalized using the $L1$ norm with N bins of histogram. The DLBP (F_{DLBP}) can be formed by the matrix concatenation of all the LBP across time points. $F_{\text{DLBP}}^{K,N} = [P_{1,j,N}, ..., P_{K,j,N}]$, $j \in \{1, ..., V\}$, where $[\cdot]$ is a matrix concatenation.

2.3.4. Textural kinetic features

The TK features have been previously employed for characterizing plaques on DCE-MRI in a rabbit model [2]. In this work, we extracted four types of textural features, including Kirsch, Sobel, Haralick, and first-order textural features to capture the plaque textures in a dynamic fashion. The detailed implementations were given in [2]. The average textural feature of plaque within a specific window size was plotted as a function of time during the period of contrast administration. A third-order polynomial was fitted to the enhancement curve to characterize its shape via a set of four model coefficients, which defined as: $\widetilde{E} = \rho_{q,3}x^3 + \rho_{q,2}x^2 + \rho_{q,1}x + \rho_{q,0}$, where $[\rho_{q,3}, \rho_{q,2}, \rho_{q,1}, \rho_{q,0}]$ are the model coefficients, representing the corresponding textural kinetic behavior of the plaque.

2.4. Voxel Level Classification

The computerized features were selected and ranked through a minimal-redundancy-maximal-relevance (mRMR) feature selection method [13], in which the optimization was driven by the mutual information quotient criterion, and then evaluated by a distance-weighted support vector machine (DWSVM) classifier [14]. The DWSVM classifier is a linear classification method with a combination of SVM and

the distance weighted discrimination (DWD) to overcome the data-piling and overfitting issues through simultaneously minimizing both the SVM and DWD loss functions. The DWSVM classifier was trained using image-derived features to distinguish vulnerable and stable plaques. In the classification, we used the best values of DWSVM parameters (C_{svm}, C_{dwd}, α) that were reported in [14].

3. EXPERIMENTAL RESULTS AND DISCUSSION

We investigated the ability of extracted image-based kinetic features on DCE-MRI to distinguish vulnerable from stable carotid plaques. We conducted two experiments to evaluate the discrimination capability of each type of kinetic features and their combinations via an iterative 10-fold cross-validation strategy. The classification task was performed on a voxel basis. To avoid a biased evaluation, we ensured that there were no voxels from the same plaque in the training and testing sets simultaneously. Four popular performance metrics, including the classification accuracy (ACC), sensitivity (SN), specificity (SP), and area under the curve of receiver operating characteristic (ROC) analysis, were computed to quantitatively measure features' ability in discriminating vulnerable and stable plaques.

Table 1 lists the classification results associated with mean (μ) and standard deviation (σ) of four measures (ACC, SN, SP, and AUC) using PK, IK, HK, TK, and their combinations in discriminating vulnerable from stable carotid plaques. The quantitative results showed that individual HK features achieved better classification performance in terms of ACC, SN, and AUC compared to the TK, PK and IK features. HK features were computed in a local and multi-resolution way, thus allowing to capture subtle, spatially proximal textural changes as well as contextual information and micro-changes during the time series. These properties are particularly appropriate for characterizing vulnerable and stable plaques having different enhancement patterns of DCE-MRI during contrast uptake. TK features also showed good performance in separating vulnerable and stable plaques with highest SP, which was consistent with the findings of [2], who showed that DCE-MRI based texture kinetic features can accurately identify vulnerable and stable plaques in the rabbit model. In addition, the results demonstrated that a combination of these kinetic features achieved better classification performance compared to the individual PK, IK, HK, and TK features. We note that Table 1 illustrates improved classification results using combined features as the number of selected features was increased till the peak performance was obtained at feature number 15 (2 PK, 3 IK, 5 HK, and 5 TK features). This is due to the fact that high-dimensional input data may overfit the training samples, thus leading to poor predictive performance in the classification. Further, more HK and TK features were chosen as the performance of classification enhanced, suggesting that HK and TK can be served as effective DCE-MRI based image signatures to distinguish vulnerable from stable carotid plaques.

Table 1. The classification performance ($\mu(\sigma)$) using individual feature types and feature combinations measured by ACC, SN, SP, and AUC. The number of features from each feature class that were selected by mRMR is given in brackets.

Feature	ACC	SN	SP	AUC
Classification using individual feature type				
PK	0.71(0.05)	0.71(0.12)	0.78(0.13)	0.80(0.06)
IK	0.72(0.11)	0.64(0.15)	0.73(0.07)	0.71(0.13)
HK	**0.81**(0.10)	**0.86**(0.07)	0.81(0.09)	**0.91**(0.05)
TK	0.79(0.09)	0.70(0.12)	**0.91**(0.04)	0.89(0.06)
Classification using feature combination				
PK(1) IK(1) HK(1) TK(2)	0.66(0.13)	0.46(0.17)	0.88(0.08)	0.80(0.07)
PK(2) IK(2) HK(4) TK(2)	0.72(0.11)	0.58(0.13)	0.86(0.07)	0.82(0.06)
PK(2) IK(3) HK(5) TK(5)	**0.86**(0.07)	0.79(0.11)	**0.93**(0.04)	**0.95**(0.03)
PK(2) IK(3) HK(8) TK(7)	0.83(0.09)	**0.81**(0.11)	0.84(0.09)	0.89(0.06)

The computation complexity was measured using the Matlab code on an Intel Core $i7$ 3.40GHz machine with a 4GB RAM. The average running times for computing PK, IK, HK, and TK were 0.02, 0.03, 1.03, and 1.25 second(s) per plaque, respectively, and the computational time of classification using 15 selected features was 0.95s for one iterative cross-validation.

4. CONCLUDING REMARKS

In this paper, we presented a kinetic feature based computerized method to discriminate between the vulnerable and the stable carotid atherosclerotic plaques with DCE-MRI. Unlike previous work focusing on PK model only or kinetic parameters calculated on texture feature curve during contrast enhancement, we studied a complementary set of image based kinetic attributes to quantitatively measure pathophysiologic changes within the plaque over the course of contrast injection. The combinations of PK, IK, HK, and TK features reflected the heterogeneity of contrast uptake between the different pathologies of vulnerable and stable plaques with various aspects of plaque microvasculature and inflammation in atherosclerosis. Further, the experimental results demonstrated that the combined feature set outperformed the individual PK, IK, HK, and TK features, suggesting that an integration of kinetic features can serve as effective imaging biomarkers for distinguishing vulnerable from stable plaque. Future work will focus on the development of a robust analysis method and validation with a large data cohort for accurate quantification of atherosclerotic plaques due to the small size of atherosclerotic plaques and to the close proximity between vessel lumen and wall,which may become a source of reciprocal signal contamination.

5. REFERENCES

[1] C.Calcagno, V.Mani, S.Ramachandran, Z.Fayad, "Dynamic contrast enhanced (DCE) magnetic resonance imaging (MRI) of atherosclerotic plaque angiogenesis," *Angiogenesis*, vol. 13, pp. 87–99, 2010.

[2] T.Wan, A.Madabhushi, A.Phinikaridou, J.Hamilton, N.Hua, T.Pham, J.Danagoulian, R.Kleiman, A.Buckler, "Spatio-temporal texture (SpTeT) for distinguishing vulnerable from stable atherosclerotic plaque on dynamic contrast enhancement (DCE) MRI in a rabbit model," *Med. Phys.*, vol. 41, no. 4, pp. 042303, 2014.

[3] H.Chen, J.Ricks, M.Rosenfeld, W.Kerwin, "Progression of experimental lesions of atherosclerosis: Assessment by kinetic modeling of black-blood dynamic contrast-enhanced MRI," *Magn. Reson. Med.*, vol. 69, no. 6, pp. 1712–1720, 2013.

[4] M.Gaens, W.Backes, S.Rozel, M.Lipperts, S.Sanders, K.Jaspers, J.Cleutjens, J.Sluimer, S.Heeneman, M.Daemen, R.Welten, J.Daemen, J.Wildberger, R.Kwee, M.Kooi, "Dynamic contrast-enhanced MR imaging of carotid atherosclerotic plaque: model selection, reproducibility, and validation," *Radiology*, vol. 266, no. 1, pp. 271–279, 2013.

[5] C.Patlak, R.Blasberg, "Graphical evaluation of blood-to-brain transfer constants from multiple-time uptake data generalizations," *J. Cereb. Blood Flow Metab.*, vol. 5, no. 4, pp. 584–590, 1985.

[6] J.Pluim, J.Maintz, M.Viergever, "Mutual-information based registration of medical images: A survey," *IEEE Trans. Medical Imaging*, vol. 22, no. 8, pp. 986–1004, 2003.

[7] W.Kerwin, M.Oikawa, C.Yuan, G.Jarvik, T.Hatsukami, "MR imaging of adventitial vasa vasorum in carotid atherosclerosis," *Magn. Reson. Med.*, vol. 59, no. 3, pp. 507–514, 2008.

[8] G.Parker, C.Roberts, A.Macdonald, G.Buonaccorsi, S.Cheung, D.Buckley, A.Jackson, Y.Watson, K.Davies, G.Jayson, "Experimentally-derived functional form for a population-averaged high-temporal-resolution arterial input function for dynamic contrast-enhanced MRI," *Magn. Reson. Med.*, vol. 56, no. 5, pp. 993–1000, 2006.

[9] N.Bhooshan, M.Giger, S.Jansen, H.Li, L.Lan, G.Newstead, "Cancerous breast lesions on dynamic contrast-enhanced MR images: Computerised characterization for image based prognostic markers," *Radiology*, vol. 254, no. 3, pp. 680–690, 2010.

[10] Y.Zheng, S.Englander, S.Baloch, E.Zacharaki, Y.Fan, M.Schnall, D.Shen, "STEP: Spatiotemporal enhancement pattern for MR-based breast tumor diagnosis," *Med. Phys.*, vol. 36, no. 7, pp. 3192–3204, 2009.

[11] J.Jesberger, N.Rafie, J.Duerk, J.Sunshine, M.Mendez, S.Remick, J.Lewin, "Model-free parameters from dynamic contrast-enhanced-MRI: sensitivity to EES volume fraction and bolus timing," *J. Magn. Reson. Imaging*, vol. 24, no. 3, pp. 586–594, 2006.

[12] T.Wan, B.Bloch, D.Plecha, C.Thompson, H.Gilmore, C.Jaffe, L.Harris, A.Madabhushi, "A radio-genomics approach for identifying high risk estrogen receptor-positive breast cancers on DCE-MRI: Preliminary results in predicting Oncotypedx risk scores," *Sci. Rep.*, vol. 18, no. 6, pp. 21394, 2016.

[13] H. Peng, F.Long, C.Ding, "Feature selection based on mutual information: Criteria of max-dependency, max-relevance, and min-redundancy," *IEEE Trans. Pattern Anal. Mach. Intell.*, vol. 27, no. 8, pp. 1226–1238, 2005.

[14] X.Qiao, L.Zhang, "Distance-weighted support vector machine," *Statistics and Its Interface*, vol. 8, pp. 331–345, 2015.